Centrality-Based Signal Detection and PSO-Optimized Estimation for Vehicular Social Networks

Yi Li, Anzhe Zhang, Shuangshuang Han, Martin Ferenc Dömény, and Guiyang Luo

***Abstract*—With the rapid advancement of the automotive industry, the demand for vehicle-centric communication continues to grow. In vehicular ad hoc networks (VANETs), the interactions among vehicles can be modeled as a social network. This paper explores the social dynamics of such networks by analyzing the eigenvector centrality of vehicles and classifying communication levels based on their centrality rankings. To support this analysis, a communication system is designed using a multiple-input multiple-output (MIMO) orthogonal frequency division multiplexing framework, incorporating the derived communication levels. Within this system, a particle swarm optimization (PSO) algorithm is employed to optimize a radial basis function (RBF) neural network for channel estimation. This approach significantly improves performance, achieving a bit error rate (BER) below 10^{-4} at relatively low signal-to-noise ratios (SNRs). Moreover, the proposed method enables the system to approach the theoretical channel capacity limit under low SNR conditions. The communication level detection method presented in this work also achieves 100% accuracy across various signal detection techniques. Overall, the proposed signal detection framework offers promising potential for enhancing the performance and reliability of future vehicular communication systems.**

***Index Terms*—Vehicular ad hoc network, social network analysis, signal detection technology, channel estimation, radial basis function neural network, particle swarm optimization algorithm, bit error rate, channel capacity**

I. Introduction

VEHICULAR ad hoc networks (VANETs) are pivotal for intelligent transportation systems, enabling real-time information sharing through vehicle-to-vehicle (V2V) and vehicle-to-infrastructure (V2I) communications [1, 2]. However, the high mobility and dynamic topology of VANETs pose significant challenges for reliable communication, particularly in achieving accurate signal detection under multipath fading and low signal-to-noise ratio (SNR) conditions [3–5].

Social network analysis (SNA) offers a promising lens to model and optimize these interactions by treating vehicles as nodes in a social graph. Analyzing metrics like eigenvector centrality can reveal a vehicle's influence, allowing for communication prioritization and efficient resource allocation [6, 7]. Concurrently, machine learning techniques, particularly radial basis function (RBF) neural networks, have demonstrated strong capabilities in channel estimation due to their superior nonlinear fitting. Yet, their performance is highly dependent on parameter selection [8, 9]. Particle swarm optimization (PSO), a robust global optimization algorithm, is well-suited to fine-tune these parameters and enhance estimation accuracy [10, 11].

While SNA, RBF, and PSO have been explored individually in VANETs, no existing work integrates these three aspects to address the joint challenge of social-aware classification and robust channel estimation. This paper fills this gap by proposing a novel communication framework that leverages SNA for centrality-aware detection and a PSO-optimized RBF network for enhanced channel estimation.

The main contributions of this work are threefold:

(1) We construct a vehicular social network from a real-world dataset, compute the eigenvector centrality for each vehicle, and classify communication levels (CLs) based on their centrality rank. The CL is encoded and embedded into the transmission sequence.

(2) A communication system based on multiple-input multiple-output-orthogonal frequency division multiplexing (MIMO-OFDM) is constructed. At the vehicle receiver, an RBF neural network is used to estimate the complex V2V channel, and the parameters of the RBF neural network are optimized using the PSO algorithm to maximize the estimation performance of the RBF network. After recovering the transmitter sequence, the CL can be extracted.

(3) The performance of the proposed method, including the bit error rate (BER), channel capacity (CC), and CL accuracy, is analyzed and compared with existing methods.

Manuscript received: 15 May 2025; revised: 23 July 2025; accepted: 28 July 2025. *(Corresponding author: Shuangshuang Han.)*

Citation: Y. Li, A. Zhang, S. Han, M. F. Dömény, and G. Luo, Centrality-based signal detection and PSO-optimized estimation for vehicular social networks, *Int. J. Intell. Control Syst.*, 2025, 30(3), 244–252.

Yi Li, Anzhe Zhang, and Shuangshuang Han are with School of Computer and Communication Engineering, University of Science and Technology Beijing, Beijing 100083, China, and also with Key Laboratory of Marine Environmental Survey Technology and Application, Ministry of Natural Resources, Guangzhou 510300, China (e-mail: m202220822@xs.ustb.edu.cn; zaz_email@163.com; hanss@ustb.edu.cn).

Martin Ferenc Dömény is with Research and Innovation Center, Óbuda University, Budapest 1034, Hungary (e-mail: domeny.martin@uni-obuda.hu).

Guiyang Luo is with State Key Laboratory of Networking and Switching Technology, Beijing University of Posts and Telecommunications, Beijing 100876, China, and also with Key State Laboratory of Integrated Services Networks, Xidian University, Xi'an 710071, China (e-mail: luoguiyang@bupt.edu.cn).

Digital Object Identifier 10.62678/IJICS202509.10236

The structure of this paper is as follows. Section II reviews the related research on signal detection technology. Section III details the modeling of SNA in VANETs comminication. Section IV details the design of the PSO-optimized RBF neural network, and provides a detailed explanation of the signal processing from the transmitter to the receiver. Section V validates the effectiveness of the proposed method through simulation experiments. Section VI summarizes this paper.

II. Related Work

Research on VANETs has increasingly leveraged insights from SNA, signal processing, and machine learning to address its unique challenges.

The application of SNA to VANETs has yielded valuable approaches for optimizing network performance. Studies have explored SNA for enhancing privacy protection through social-aware mechanisms [12], improving information dissemination efficiency by predicting content propagation paths [13], and developing multi-layer network models that integrate social and communication links for superior routing [14]. These works demonstrate the potential of social relationships to inform network optimization, yet they do not explicitly integrate these social metrics into the physical layer signal detection process.

On the signal detection front, research has focused on overcoming the impairments of high-mobility environments. Key efforts include developing robust synchronization and carrier frequency offset estimation methods for new radio vehicle-to-everything (NR-V2X) systems [15–18], as well as exploring the integration of sensing and communication (ISAC) to improve spectral efficiency [19, 20]. While these methods enhance reliability, they operate independently of the social context of the communicating vehicles.

Recently, deep learning (DL) has emerged as a powerful tool for addressing complex challenges in wireless communications. DL-based approaches have been successfully applied to channel estimation [21] and end-to-end signal detection [22], often surpassing traditional algorithms. To mitigate the high computational and data requirements of DL, techniques like transfer learning have been introduced to reduce training overhead [23, 24]. However, the combination of SNA with efficient, lightweight neural networks like RBF, optimized by bio-inspired algorithms, such as PSO, remains an unexplored area.

In summary, existing research has progressed along three parallel tracks: SNA for network-layer optimization, advanced signal processing for physical-layer reliability, and DL for data-driven modeling. Our work distinguishes itself by synthesizing these strands. We leverage SNA to derive communication priorities, which are embedded into the physical layer signal, and employ a PSO-optimized RBF network for efficient and highly accurate channel estimation, thereby bridging the gap between social context and physical layer performance.

III. Social Network Analysis in VANET Communication

A. Definition of Social Network Analysis

In SNA, social networks are typically modeled as a mathematical graph $G=(V,E)$, where V denotes a set of vertices representing social actors, and E denotes a set of edges representing the relationships between them [25]. Each edge connects two nodes and can represent various types of relationships, which may be multidimensional and directional [26]. This abstraction simplifies a social network into points and lines, where points correspond to entities and lines correspond to their interactions.

B. Key Node Measurement Indicator

Eigenvector centrality is a measure of node importance based on the structure of a network [27]. It is based on the assumption that the importance of a node is not only determined by the number of nodes it is directly connected to, but also by the importance of those connected nodes. Specifically, if a node is connected to many important nodes, the node itself is considered to be important.

Assuming we have a network with an adjacency matrix A, where $A_{ij}=1$ indicates that there is a connection between node i and node j, and $A_{ij}=0$ otherwise [25]. Eigenvector centrality x is a vector, where each element x_i represents the centrality of node i. Eigenvector centrality satisfies the following equation

$$Ax=\lambda x \tag{1}$$

where λ is the largest eigenvalue of the adjacency matrix A, and x is the corresponding eigenvector. This equation means that the centrality of each node is the weighted sum of the centralities of the nodes it is connected to, scaled by a constant λ.

Specifically, for each node i, its eigenvector centrality x_i can be expressed as

$$x_i=\frac{1}{\lambda}\sum_{j=1}^{n}A_{ij}x_j \tag{2}$$

where n is the total number of nodes in the network, and A_{ij} is the element of the adjacency matrix, indicating the connection between node i and node j. This formula shows that the centrality of node i is the weighted sum of the centralities of all nodes connected to it, with the weights determined by the adjacency matrix.

To calculate eigenvector centrality, we need to solve for the largest eigenvalue λ of the adjacency matrix A and the corresponding eigenvector x [26]. This can typically be done using numerical methods such as the power iteration method. After obtaining the eigenvector, it is usually normalized so that the sum of all node centralities equals 1.

C. Determining Communication Level

The computed eigenvector centrality values for all vehicles are sorted in descending order. Based on their percentile ranking, vehicles are classified into four distinct CLs: A (highest influence), B, C, and D (lowest influence). This classification is then encoded into a 2-bit binary sequence (00, 01, 10, and 11, respectively) and appended to the vehicle's transmission data. This allows the communication system to prioritize messages based on the social importance of the sender, optimizing network resource allocation.

IV. System Model

In calculating the social relationship strength (SRS) between vehicles, we utilize data from the OpenData V11.0-vehicle reidentification dataset VRID-1. The dataset originates from a city's card point, captured by 326 high-definition cameras over a period of 14 days, covering daytime. The dataset includes images of the 10 most common vehicle models, totaling 10,000 images. Each vehicle model has 100 different vehicle identities (IDs), which means 100 different vehicles. Additionally, each vehicle ID contains 10 images, with these 10 images taken at different road card points. From the description above, it is easy to deduce that the dataset contains 1000 different vehicle images, forming a social relationship network. These images come from various card points, and due to the absence of card point information, we randomly assign card point information to each image. We take the average of the results from the 326 cameras over 14 days, which is approximately 23 cameras. We can interpret this as having 1 camera at each of the 23 card points.

A. Calculation of SRS Considering Eigenvector Centrality

First, we import the node table and edge table into the software. The node table is shown in Table 1, and the edge table is shown in Table 2. Table 1 has three columns: vehicle ID, vehicle label, and vehicle category. Table 2 has four columns: source, target, type, and weight. We consider two vehicles captured by the same camera as a source-target pair. Both source and target represent the vehicle ID. To enrich the vehicle network, there are two types of edges: directed and undirected. The weight of the edges ranges from 1 to 10.

Table 1 Node table for 1000 vehicles in the dataset.

ID	Label	Category
1	1	B
2	2	A
3	3	B
4	4	A
5	5	C
6	6	C
7	7	C
8	8	B
9	9	C
⋮	⋮	⋮
1000	1000	A

After conducting a comprehensive analysis of this social network, we choose eigenvector centrality as the measure of the SRS. As shown in Table 3, it concludes the eigenvector centrality of 1000 vehicles.

After calculating the SRS, we then proceed to categorize the CL within the social network of vehicle 1. First, we sort the SRS values of the 1000 vehicles from the highest to lowest and divide them into four intervals, corresponding to CL A, B, C, and D. Then, we encode the CL A, B, C, and D as 00, 01, 10, and 11, respectively, to be part of the sender's sequence.

Table 2 Edge table for 1000 vehicles in the dataset.

Source	Target	Type	Weight
1	2	Directed	4
1	12	Undirected	10
1	16	Undirected	3
1	24	Undirected	1
1	51	Undirected	10
1	55	Undirected	3
1	71	Undirected	7
1	75	Undirected	1
1	82	Directed	8
⋮	⋮	⋮	⋮
999	1000	Undirected	7

Table 3 Eigenvector centrality of 1000 vehicles.

ID	Label	Category	Eigenvector centrality
1	1	B	0.370991
2	2	A	0.370991
3	3	B	0.219883
4	4	A	0.197522
5	5	C	0.410916
6	6	C	0.219883
7	7	C	0.197522
8	8	B	0.244550
9	9	C	0.614061
⋮	⋮	⋮	⋮
1000	1000	A	0.370991

B. Signal Detection Method Based on MIMO-OFDM System in VANET

As shown in Fig. 1, the first step is to conduct an SNA on a vehicular network consisting of 1000 vehicles, considering both node and network dimensions. After comprehensive analysis, we use the eigenvector centrality value as the measure of social relationship strength. In the proposed MIMO-OFDM system, the CL derived from eigenvector centrality is encoded into a 2-bit sequence and appended to the transmitted data frame after pilot insertion. This allows the receiver to not only estimate the channel and recover the data, but also extract the CL information for social-aware resource allocation. Based on the magnitude of social relationship strength, we categorize the CL into four grades: A, B, C, and D, which are encoded as 00, 01, 10, and 11, respectively. The 2-bit CL is appended to the end of the sequence after the insertion of pilots. Subsequently, the bit stream to be transmitted is transformed into multiple input data streams to achieve output through multiple antennas. For each signal path, processes such as pilot insertion, CL insertion, serial-to-parallel conversion, inverse fast fourier transform (IFFT), addition of cyclic prefix, and parallel-to-serial conversion are performed.

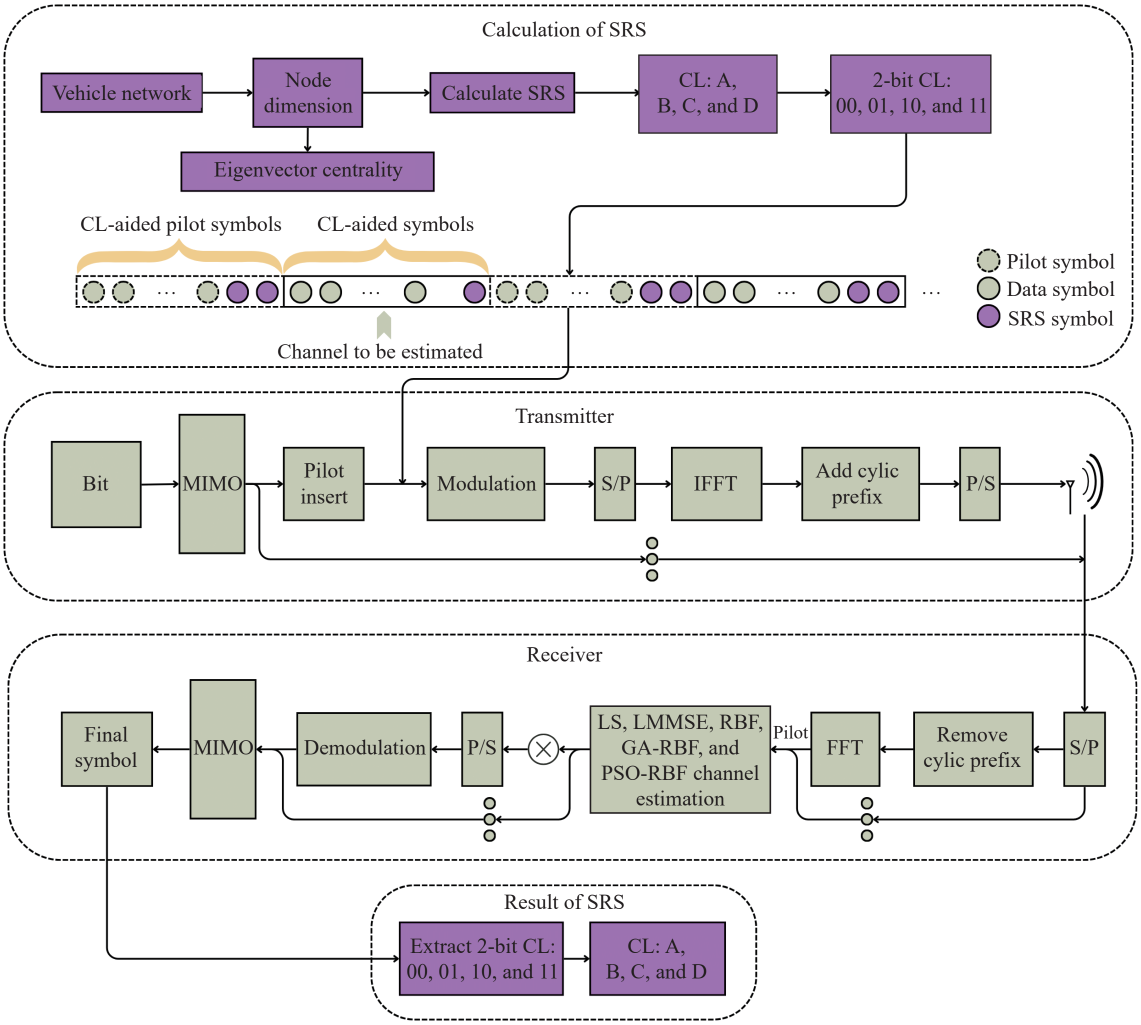

Fig. 1 Vehicular network communication system model based on SRS and MIMO-OFDM.

When the signal reaches the receiving end, each signal path undergoes serial-to-parallel conversion, removal of cyclic prefix, fast fourier transform (FFT), channel estimation based on pilots, and parallel-to-serial conversion, among other processes. Finally, the multiple signals are combined to be a sequence containing pilots, messages, and CL. The 2-bit CL can be extracting from the end of the sequence.

At the transmitter, we first split the initial sequence. Then, the same operations are performed on each signal path. The first step is to insert pilot signals, which are known reference signals embedded in specific subcarriers. They are uniformly distributed across the frequency band to support accurate channel estimation. Then, we insert the 2-bit symbols representing the CL into the sequence.

Next, the sequence is modulated, and in this case, we use quadrature phase shift keying (QPSK) modulation. QPSK is a digital modulation technique that conveys data by changing the phase of a carrier signal. The mathematical expression for QPSK is

$$s(t) = I(t)\cos(2\pi f_c t) - Q(t)\sin(2\pi f_c t) \tag{3}$$

where $I(t)$ and $Q(t)$ are the baseband signals, and f_c is the carrier frequency.

Then, we perform a serial-to-parallel conversion on the sequence, breaking down the bit-by-bit serial data into multiple parallel data bits for IFFT processing. In OFDM systems, the IFFT operation is crucial for converting frequency-domain symbols into a time-domain signal. The process begins with modulated data symbols that are assigned to multiple orthogonal subcarriers, forming the input to the IFFT. The IFFT then transforms these frequency-domain symbols into a time-domain signal, creating the OFDM symbol that is transmitted over the channel. This operation is essential because it allows OFDM to efficiently distribute data across multiple subcarriers, reducing the impact of multipath interference and frequency-selective fading.

To reduce the effects of multipath propagation and intersymbol interference, we add a cyclic prefix to the sequence. Specifically, a segment of data from the end of the OFDM symbol is copied and placed at the beginning of the symbol. Subsequently, the multiple parallel data bits are combined into a serial data stream for bit-by-bit transmission over a single line. Up to this point, the sequence processing at the transmitter is completed.

When the signal reaches the receiving end, each signal path undergoes serial-to-parallel conversion, removal of cyclic prefix. Next, the sequence is processed with the FFT. In OFDM systems, the FFT is a crucial operation at the receiver, used to convert the received time-domain signal back to the frequency domain. The mathematical formula for the FFT is

$$X[k] = \sum_{n=0}^{N-1} x[n] \cdot \mathrm{e}^{-j\frac{2\pi}{N}kn},\ k = 0, 1, \ldots, N-1 \tag{4}$$

where $X[k]$ represents the frequency-domain signal, $x[n]$ is the time-domain signal, j is the imaginary unit, and N is the length of the FFT. This allows the receiver to obtain the channel's frequency response and perform equalization to recover the original data symbols. The efficient implementation of the FFT is vital for the performance of OFDM systems.

Next, we perform channel estimation on the signal after the FFT transform. The specific principles of the least square (LS) [28], linear minimum mean square error (LMMSE) [28], RBF [29], and genetic algorithm (GA)-optimized RBF [29] channel estimation algorithms have been explained in existing research. This paper focuses on introducing the channel estimation algorithm based on the RBF neural network optimized by the PSO algorithm.

The PSO-optimized RBF neural network channel estimation algorithm is a method that combines intelligent optimization algorithms with neural networks to enhance the accuracy and efficiency of channel estimation.

The RBF neural network consists of an input layer, a hidden layer, and an output layer. The hidden layer uses Gaussian functions as radial basis functions

$$\phi_i(x) = \exp\left(-\frac{\|x - c_i\|^2}{2\sigma_i^2}\right) \tag{5}$$

where c_i is the center and σ_i is the width. The network output is calculated as

$$y(x) = \sum_{i=1}^{n} w_i \cdot \phi_i(x) \tag{6}$$

where w_i represents the weights.

PSO optimizes the parameters of the RBF network by iteratively updating the velocity and position of particles. The particle position update formulas are

$$v_{i,d}^{t+1} = \omega v_{i,d}^{t} + c_1 r_1 (p_{i,d} - x_{i,d}^{t}) + c_2 r_2 (p_{g,d} - x_{i,d}^{t}) \tag{7}$$

$$x_{i,d}^{t+1} = x_{i,d}^{t} + v_{i,d}^{t+1} \tag{8}$$

where ω is the inertia weight, c_1 and c_2 are learning factors, r_1 and r_2 are random numbers, $p_{i,d}$ is the individual optimal position, and $p_{g,d}$ is the global optimal position.

The loss function for channel estimation typically uses the mean squared error

$$J = \frac{1}{2} \sum_{k=1}^{K} \|y_k - \hat{y}_k\|^2 \tag{9}$$

where y_k is the actual channel output, $\hat{y}_k$ is the estimated channel output, and K is the number of samples.

Algorithm workflow can be summarized as follows:

- Randomly initialize the centers c_i, widths σ_i, and weights w_i of the RBF network.
- Set the swarm size, inertia weight ω, learning factors c_1 and c_2, and the maximum number of iterations.
- Calculate the fitness (loss function J) for each particle. Update the individual optimal solution $p_{i,d}$ and the global optimal solution $p_{g,d}$. Adjust the particle velocity and position using the PSO update formulas. Update the parameters of the RBF network with the new particle positions.
- Stop when the maximum number of iterations is reached or the loss function J converges.
- Output the final RBF network parameters and channel estimation results.

PSO optimizes the parameters c_i, σ_i, and w_i of the RBF network, iteratively minimizing the loss function J to gradually improve the performance of channel estimation.

After channel estimation, the signal is converted from parallel to serial and demodulated via QPSK. This process down-converts the received signal to recover the in-phase and quadrature components, which are then mapped to the nearest constellation points to retrieve the original binary data.

Finally, the multiple signals are combined to obtain a sequence containing pilots, messages, and CL. The 2-bit CL can be extracted from the end of the sequence.

V. SIMULATION EXPERIMENT

The signal detection process is detailed in Algorithm 1, which combines SRS-based detection with PSO-optimized RBF neural networks. The algorithm begins by initializing key communication parameters and generating the CL based on vehicle centrality. It then carries out signal transmission and reception, incorporating steps such as pilot and CL insertion, IFFT/FFT operations, and channel estimation using multiple techniques. The BER and channel capacity are computed over a range of SNR levels. After several iterations, the algorithm averages the BER and channel capacity to ensure robust performance evaluation.

Table 4 presents the simulation parameters used for the communication system and optimization algorithms. The communication setup includes two transmit and two receive antennas, QPSK modulation, an IFFT length of 64, 50 subcarriers, 12 symbols per subcarrier, two bits per symbol, and a cyclic prefix of length eight. The RBF neural network comprises 12 input neurons, 64 hidden neurons, and 12 output neurons. For optimization, GA uses a population size of 10, a mutation probability of 0.1, and a crossover probability of 0.6. The PSO algorithm is configured with a population size of 10, a maximum of 40 iterations, an inertia weight of 0.5, cognitive and social coefficients of 1.5, and an initial position range of [0.00, 0.02].

The effectiveness of our proposed method is evaluated by its bit BER, a key reliability metric, and by examining the performance gains achieved through the use of relay nodes to enhance signal quality and extend communication range.

Fig. 2 illustrates the BER performance of the proposed method alongside four channel estimation techniques over an SNR range from −8 to 20 dB. As shown in Fig. 2, the performance gap between the LS and LMMSE methods is relatively small. However, LMMSE achieves slightly better BER due to its ability to minimize mean square error and more effectively suppress noise. The RBF neural network based channel estimation outperforms both LS and LMMSE, particularly at higher SNR levels. Once the SNR exceeds approximately 10 dB, the RBF-based method shows a marked improvement, reducing the BER to nearly 10^{-3} at 20 dB.

Algorithm 1 SRS-based signal detection algorithm with PSO-optimized RBF

```
Generate SRS and CL
for i = 1 to 1000 (vehicle number) do
    x_i = (1/λ) Σ_{j=1}^{n} A_ij x_j,  j = 1,2,...,n = 1000
    get eigenvector centrality of vehicle i in 1000 vehicles
end for
Determine the CL A, B, C, and D based on eigenvector centrality.
Encode the CL as 00, 01, 10, and 11, and attach them to the end of the
  OFDM symbol.
Get BER, CC, and CL
for i = 1 to 500 (to average) do
    Transmitter: pilot insertion, CL insertion, serial-to-parallel
      conversion, IFFT, addition of cyclic prefix, and parallel-to-serial
      conversion.
    for i = −8 to 20 (SNR) do
        Receiver: serial-to-parallel conversion, removal of cyclic prefix,
          FFT, channel estimation based on pilots, and parallel-to-serial
          conversion. The channel estimation methods include LS,
          LMMSE, RBF, GA-optimized RBF, and PSO-optimized RBF.
        Extract CL and calculate BER
        Compute capacity(:, tt) = 0.5 × log10(1 + SNR(linear) × BER(:, tt))
    end for
    Get 500 CL and BER from −8 to 20 dB.
    Get 500 CC from −8 to 60 dB.
end for
Average 500 BER over a range of −8 to 20 dB. Take the CL that occurs
  the most times under each SNR. Average 500 CC over a range of −8 to
  60 dB.
```

After optimizing the RBF network parameters using GA and PSO, the BER performance shows a significant improvement beyond an SNR of approximately 10 dB. At 20 dB, GA reduces the BER to around 10^{-4}, while PSO achieves a comparable BER of 10^{-4} at approximately 19 dB. This indicates that PSO slightly outperforms GA in optimizing the RBF network. The superior performance of PSO is attributed to its faster convergence to the global optimum, as well as its high computational efficiency and adaptability in dynamic environments. In particular, PSO achieves comparable optimal performance with an SNR approximately 6 dB lower than that required by GA, further highlighting its effectiveness.

Fig. 3 presents the analysis of CL detection. As shown, the proposed CL detection method utilizes the characteristics of OFDM frequency division multiplexing to analyze the CL results of parallel transmission, selects the CL with the most occurrences, and achieves 100% recognition accuracy in various channel estimations. Although there are some erroneous values in the simulation experiments, since each result goes through approximately 500 iterations, in order to fully utilize these values, a relatively high CL was achieved after statistically averaging these iterative values. This high accuracy is attributed to the comprehensive utilization of each detection dataset and the efficient processing of detection outcomes. By analyzing the detected communication levels, the algorithm reliably determines the most probable CL. In

Table 4 Simulation parameters.

Parameter	Value
Transmitting antenna	2
Receiving antenna	2
Carrier	50
Bit per symbol	2
Learning rate	0.1
Crossover probability (GA)	0.6
Cognitive coefficient (PSO)	1.5
Cyclic prefix	8
IFFT length	64
Symbol per carrier	12
Interval	5
Popsize (GA and PSO)	10
Inertia weight (PSO)	0.5
Social coefficient (PSO)	1.5
Modulation type	QPSK
Input layer neuron	12
Hidden layer neuron	64
Output layer neuron	12
Mutation probability (GA)	0.1
Maximum iteration (PSO)	40
Initial position range (PSO)	[0.00, 0.02]

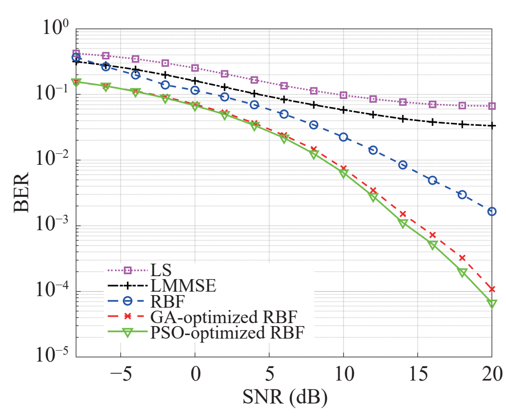

Fig. 2 BER performance in a multipath channel without a relay, including the CL of vehicle 9, with 2 transmit and receive antennas.

Fig. 3, the detection results for vehicles 9, 1, 3, and 15 are shown, corresponding to CL levels A, B, C, and D, respectively. For clarity, the vertical axis represents the encoded CL levels as 0, 1, 2, and 3. Across the SNR range from −8 to 20 dB, the detection results obtained using five different channel estimation methods, including the PSO-based method, are fully consistent with the ground truth levels.

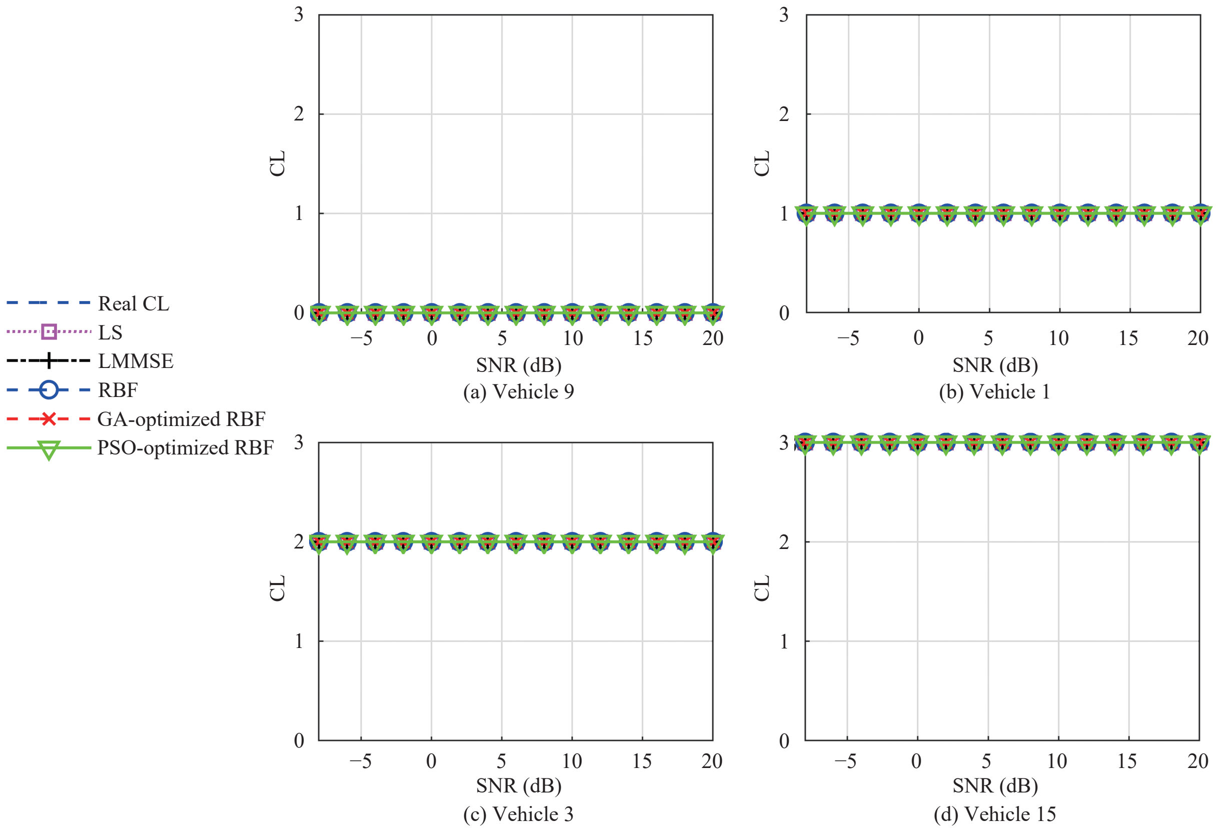

Fig. 3 CL in a multipath channel. CLs for vehicles 1, 3, 9, and 15 correspond to four different CLs, respectively. The number of transmit and receive antennas is two.

We also analyzed the channel capacity of the proposed communication system, as illustrated in Fig. 4, using the detection results of vehicle 9 as a representative example. To thoroughly evaluate the performance of various detection methods, the SNR range was extended from −8 to 60 dB. Under these conditions, the theoretical maximum channel capacity of the system is three. As expected, the channel capacity increases with SNR and gradually approaches this limit.

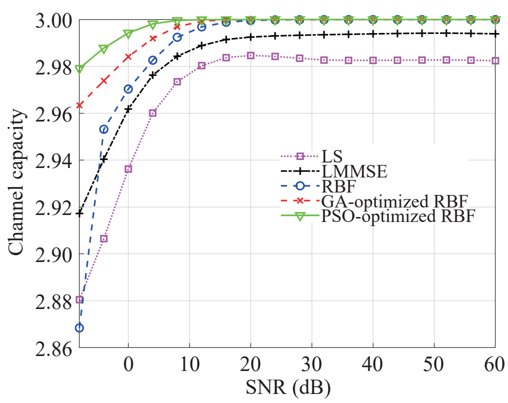

Fig. 4 CC in a multipath channel without a relay, including the CL of vehicle 9, with 2 transmit and receive antennas.

Overall, the proposed signal detection method demonstrates superior performance under low SNR conditions and approaches the channel capacity at a lower SNR than the other three methods. Specifically, the GA exhibits a slower convergence, requiring approximately 4 dB more SNR than the PSO method to achieve the capacity limit. The RBF neural network without optimization also reaches the limit, though not as efficiently. In contrast, the LS and LMMSE methods converge to slightly lower capacity values, falling short of the theoretical maximum.

VI. Conclusion

The proposed signal detection method, combining SRS-based detection with a PSO-optimized RBF neural network, demonstrates substantial improvements in both bit error rate performance and channel capacity. The method achieves a BER close to 10^{-4} at an SNR of 19 dB. The integration of relays enhances system performance by enabling the PSO-based method to attain optimal results at lower SNR levels.

In terms of channel capacity, the proposed approach achieves the channel capacity limit at a lower SNR compared to the benchmark methods, particularly under low-SNR conditions. The PSO algorithm proves especially effective, achieving this limit at an SNR of around 5 dB. Furthermore, the CL detection method achieves 100% accuracy across all tested signal detection techniques, ensuring reliable classification and prioritization of messages within vehicular social networks.

By enabling accurate detection of communication priority, the proposed framework supports efficient resource allocation, reduces network congestion, and improves overall user experience. These results affirm the method’s potential as a robust and efficient solution for future vehicular communication systems, offering strong performance, scalability, and suitability for real-world deployment. Continued research may further enhance its adaptability and integration into intelligent transportation infrastructures.

Acknowledgment

This work was supported by the Open Fund Project of Key Laboratory of Marine Environmental Survey Technology and Application, Ministry of Natural Resources (No. MESTA-2024-B004).

References

[1] F.-Y. Wang, From RAG/RAT to SAGE for social transportation: A CoT and new perspective on smart logistics and mobility, *IEEE Trans. Intell. Veh.*, 2024, 9(6), 5005–5008.

[2] B. Lu, Q. Miao, Y. Liu, T. S. Tamir, H. Zhao, X. Zhang, Y. Lv, and F.-Y. Wang, A diffusion model for traffic data imputation, *IEEE/CAA J. Autom. Sin.*, 2025, 12(3), 606–617.

[3] H. T. Nguyen, M. Noor-A-Rahim, Y. L. Guan, and D. Pesch, Cellular V2X communications in the presence of big vehicle shadowing: Performance analysis and mitigation, *IEEE Trans. Veh. Technol.*, 2023, 72(3), 3764–3776.

[4] S. Han, Y. Bai, T. Zhang, Y. Chen, and C. Tellambura, Parallel management of IoV information enabled by blockchain and decentralized autonomous organizations, *IEEE Trans. Intell. Veh.*, 2024, 9(4), 4759–4768.

[5] Y. Zhu, W. Tong, Y. Hu, B. Han, R. F. Schaefer, and A. Schmeink, Joint redundancy and blocklength allocation for secure-reliability performance optimization in future V2X networks, *IEEE Trans. Veh. Technol.*, 2024, 73(12), 19826–19831.

[6] S. Khan, F. Luo, Z. Zhang, M. A. Rahim, S. Khan, S. F. Qadri, and K. Wu, A privacy-preserving and transparent identity management scheme for vehicular social networking, *IEEE Trans. Veh. Technol.*, 2022, 71(11), 11555–11570.

[7] Y. Zhao, W. Liu, B. Li, X. Zhou, Z. Ning, T. Qiu, and M. Atiquzzaman, Entity and sociality trust-aware model for content distribution in social internet of vehicles, *IEEE Trans. Veh. Technol.*, 2022, 71(12), 12511–12522.

[8] J. Chen, J. Zhang, N. Zhao, Y. Pei, Y.-C. Liang, and D. Niyato, Joint device participation, dataset management, and resource allocation in wireless federated learning via deep reinforcement learning, *IEEE Trans. Veh. Technol.*, 2024, 73(3), 4505–4510.

[9] S. Han, Y. Li, T. Zhang, Y. Bai, Y. Chen, and C. Tellambura, Signal detection techniques in social internet of vehicles: Review and challenges, *IEEE Intell. Transp. Syst. Mag.*, 2025, 17(2), 79–94.

[10] L. Lei, T. Liu, K. Zheng, and L. Hanzo, Deep reinforcement learning aided platoon control relying on V2X information, *IEEE Trans. Veh. Technol.*, 2022, 71(6), 5811–5826.

[11] X. Xing, Z. Zhou, Y. Li, B. Xiao, and Y. Xun, Multi-UAV adaptive cooperative formation trajectory planning based on an improved MATD3 algorithm of deep reinforcement learning, *IEEE Trans. Veh. Technol.*, 2024, 73(9), 12484–12499.

[12] B. Ying and A. Nayak, A distributed social-aware location protection method in untrusted vehicular social networks, *IEEE Trans. Veh. Technol.*, 2019, 68(6), 6114–6124.

[13] H. Zhang, S. Huang, X. Wang, J. Li, X. Wang, and V. C. M. Leung, A measurement-driven analysis and prediction of content propagation in the device-to-device social networks, *IEEE Trans. Knowl. Data Eng.*, 2023, 35(8), 7651–7664.

[14] Z. Lu, Y. E. Sagduyu, and Y. Shi, Integrating social links into wireless networks: Modeling, routing, analysis, and evaluation, *IEEE Trans. Mob. Comput.*, 2019, 18(1), 111–124.

[15] Y.-H. You, Y.-A. Jung, S.-H. Lee, H.-G. Song, S.-C. Choi, and H.-K. Song, Group-wise sidelink synchronization signal and carrier frequency offset detection method for D2D-based NR-V2X systems, *IEEE Internet Things J.*, 2022, 9(4), 2973–2983.

[16] Y. Li, C. Hao, Y. Xie, and S. Han, Computational experiments and comparative analysis of signal detection algorithms in vehicular ad hoc networks, *IEEE J. Radio Freq. Identif.*, 2024, 8, 402–411.

[17] Y. Li, S. Han, Y. Chen, and L. Du, Computational experiments of signal detection algorithms in VANETs based on parallel intelligence, in *Proc. 2023 IEEE 3rd International Conference on Digital Twins and Parallel Intelligence (DTPI)*, Orlando, FL, USA, 2023, 1–4.

[18] N. Decarli, S. Bartoletti, A. Bazzi, R. A. Stirling-Gallacher, and B. M. Masini, Performance characterization of joint communication and sensing with beyond 5G NR-V2X sidelink, *IEEE Trans. Veh. Technol.*, 2024, 73(7), 10044–10059.

[19] A. Gao, Z. Zhu, J. Zhang, W. Liang, and Y. Hu, Matching combined heterogeneous multi-agent reinforcement learning for resource allocation in NOMA-V2X networks, *IEEE Trans. Veh. Technol.*, 2024, 73(10), 15109–15124.

[20] W. Xu, F. Gao, X. Tao, J. Zhang, and A. Alkhateeb, Computer vision aided mmWave beam alignment in V2X communications, *IEEE Trans. Wireless Commun.*, 2023, 22(4), 2699–2714.

[21] B. Wang, K. Xu, S. Zheng, H. Zhou, and Y. Liu, A deep learning-based intelligent receiver for improving the reliability of the MIMO wireless communication system, *IEEE Trans. Reliab.*, 2022, 71(2), 1104–1115.

[22] H. Safi, I. Tavakkolnia, and H. Haas, Deep learning based end-to-end optical wireless communication systems with autoencoders, *IEEE Commun. Lett.*, 2024, 28(6), 1342–1346.

[23] H.-P. Yin, X.-H. Zhao, J.-L. Yao, and H.-P. Ren, Deep-learning-based channel estimation for chaotic wireless communication, *IEEE Wireless Commun. Lett.*, 2024, 13(1), 143–147.

[24] N. Van Huynh and G. Li, Transfer learning for signal detection in wireless networks, *IEEE Wireless Commun. Lett.*, 2022, 11(11), 2325–2329.

[25] Y. Wang, H. Sun, Y. Zhao, W. Zhou, and S. Zhu, A heterogeneous graph embedding framework for location-based social network analysis in smart cities, *IEEE Trans. Ind. Inform.*, 2020, 16(4), 2747–2755.

[26] E. Sahafizadeh and B. Tork Ladani, A model for social communication

network in mobile instant messaging systems, *IEEE Trans. Comput. Soc. Syst.*, 2020, 7(1), 68–83.

[27] H. Aksu, I. Korpeoglu, and O. Ulusoy, An analysis of social networks based on tera-scale telecommunication datasets, *IEEE Trans. Emerg. Top. Comput.*, 2019, 7(2), 349–360.

[28] Z. Chen, Q. Yao, Y. Zhong, J. Ye, and X. Ge, Efficient spatial channel estimation in extremely large antenna array communication systems: A subspace approximated matrix completion approach, *IEEE Open J. Commun. Soc.*, 2025, 6, 1216–1230.

[29] F. Peng and X. Chen, An efficient optimization method for antenna arrays using a small population diploid genetic algorithm based on local RBF networks, *IEEE Trans. Antennas Propag.*, 2024, 72(4), 3237–3249.

Yi Li received the BS degree in electronic information engineering from Tianjin University of Science and Technology, Tianjin, China, in 2022. He is currently pursuing the MS degree in communication engineering at School of Computer and Communication Engineering, University of Science and Technology Beijing, Beijing, China. His research interests include Internet of Vehicles and vehicular communications.

Anzhe Zhang received the BS degree in communication engineering from South-Central Minzu University, Wuhan, China, in 2025. He is currently pursuing the MS degree in communication engineering at School of Computer and Communication Engineering, University of Science and Technology Beijing, Beijing, China. His research interests include channel estimation.

Shuangshuang Han received the BS degree in communication engineering and the MS degree in communication and information systems from Shandong University, Jinan, China, in 2006 and 2009, respectively. She received the PhD degree from Department of Electrical and Computer Engineering, University of Alberta, Edmonton, AB, Canada, in 2013. She was an assistant professor from 2013 to 2019, and an associate professor from 2019 to 2021 at Institute of Automation, Chinese Academy of Sciences, China. Currently, she is an associate professor at School of Computer and Communication Engineering, University of Science and Technology Beijing, Beijing, China. Her research interests include wireless communications, Internet of Vehicles, and signal detection techniques.

Martin Ferenc Dömény is currently pursuing the MS degree in computer engineering at Óbuda University, Hungary. His research at the Physiological Controls Research Center focuses on the application and analysis of optimization algorithms for cancer therapy planning, including evolutionary methods such as genetic algorithms and particle swarm optimization. He has hands-on experience in mathematical modeling and the simulation of tumor dynamics. His broader interests include AI, computational biology, and the development of tools for model-based decision support in healthcare.

Guiyang Luo received the PhD degree from Beijing University of Posts and Telecommunications, Beijing, China, in 2017. He was a specially appointed associate researcher and PhD supervisor from 2020 to 2025 at State Key Laboratory of Networking and Switching Technology, School of Computer Science, Beijing University of Posts and Telecommunications, China. His research interests include multi-agent systems and machine-type communications.